



Obrabotka metallov - Metal Working and Material Science

Journal homepage: http://journals.nstu.ru/obrabotka_metallov



Optimization of selective laser melting modes of powder composition of the AlSiMg system

Natalia Saprykina^{1, a}, Valentina Chebodaeva^{2, b}, Alexandr Saprykin^{1, c}, Yuriï Sharkeev^{2, d},
Egor Ibragimov^{1, e}, Taisiya Guseva^{1, f}

¹ National Research Tomsk Polytechnic University, 30 Lenin Avenue, Tomsk, 634050, Russian Federation

² Institute of Strength Physics and Materials Sciences SB RAS, 2/4, pr. Akademicheskii, Tomsk, 634055, Russian Federation

^a  <https://orcid.org/0000-0002-6391-6345>,  saprikina@tpu.ru; ^b  <https://orcid.org/0000-0002-1980-3941>,  vtina5@mail.ru;

^c  <https://orcid.org/0000-0002-6518-1792>,  sapraa@tpu.ru; ^d  <https://orcid.org/0000-0001-5037-245X>,  sharkeev@ispms.tsc.ru;

^e  <https://orcid.org/0000-0002-5499-3891>,  egor83rus@tpu.ru; ^f  <https://orcid.org/0000-0002-3285-1673>,  tsh2@tpu.ru

ARTICLE INFO

Article history:

Received: 05 November 2023

Revised: 24 November 2023

Accepted: 28 December 2023

Available online: 15 March 2024

Keywords:

Selective laser melting

Metal powder

Porosity

Selective laser melting modes

Microhardness

Energy input

Alloy of the aluminum-silicon-magnesium system

Funding

The research was carried out at the expense of the grant of the Russian Science Foundation No. 22-29-01491, <https://rscf.ru/project/22-29-01491/>.

Acknowledgements

Authors would like to thank M.A. Khimich for her help in present study. The research was carried out using the equipment of the CSU NMNT TPU.

ABSTRACT

Introduction. New aluminum-based powder systems are currently being developed for additive manufacturing. The scientists' work is aimed at comprehensive studies of powder production, optimization of conditions for alloy production and formation of three-dimensional specimens with minimal porosity and absence of cracking during selective laser melting. **The purpose of this work** is the synthesis of an almost spherical Al-Si-Mg composite powder (91 wt. % Al, 8 wt. % Si, 1 wt. % Mg) from aluminum powder PA-4 (GOST 6058-22), silicon powder (GOST 2169-69) and magnesium powder MPF-4 (GOST 6001-79), which were not originally intended for selective laser melting technology. The work also provides for the optimization of selective laser melting modes to obtain an alloy and form three-dimensional specimens with minimal porosity and no cracking. To create a powder composition, powders ranging in size from 20 to 64 μm were selected by sieve analysis and subjected to mechanical mixing in a ball mill in a protective argon medium for one hour. **The research methods** are methods of X-ray diffraction and X-ray phase analysis, transmission electron microscopy, mechanical tests of microhardness. Studies of the powder composition after mechanical mixing showed that the mixed powder of aluminum, silicon and magnesium is a conglomerate of particles of spherical, oval and irregular shape. **Results and discussions.** The optimal modes for obtaining a specimen with a minimum porosity of 0.03 % and a microhardness of 1,291 MPa are selective laser melting modes: $P = 90$ W, $V = 225$ mm/s, $S = 0.08$ mm, $h = 0.025$ mm. The conducted research shows the possibility of synthesizing products from metal powders that are not adapted to processing by selective laser melting and obtaining an alloy with new mechanical properties during laser action.

For citation: Saprykina N.A., Chebodaeva V.V., Saprykin A.A., Sharkeev Y.P., Ibragimov E.A., Guseva T.S. Optimization of selective laser melting modes of powder composition of the AlSiMg system. *Obrabotka metallov (tehnologiya, oborudovanie, instrumenty) = Metal Working and Material Science*, 2024, vol. 26, no. 1, pp. 22–37. DOI: 10.17212/1994-6309-2024-26.1-22-37. (In Russian).

* Corresponding author

Saprykina Natalia A., Ph.D. (Engineering), Associate Professor
 National Research Tomsk Polytechnic University,
 30 Lenin Ave.,
 634050, Tomsk, Russian Federation
 Tel.: +7 923 49-72-483, e-mail: saprikina@tpu.ru

Introduction

Aluminum-based alloys, due to its light weight, high strength, ductility and good corrosion resistance, are widely used in many branches of mechanical engineering [1, 2].

Aluminum is almost three times lighter than steel and is the third most abundant element on Earth. Traditional methods for producing parts from aluminum alloys are: pressure casting, gravity die casting, green sand casting [2].

In recent years, additive manufacturing (*AM*) has revolutionized the manufacturing industry as it has made possible to manufacture parts of complex geometric shapes directly from a 3-dimensional drawings [3, 4]. The software slices the 3D object into layers, which thickness ranges from 20 to 100 μm , while the laser moves along the predetermined trajectory and fuses layer by layer. The most common technology for layer-by-layer parts production from metal powders is selective laser melting (*SLM*) technology.

An analysis of the literature shows that alloys based on iron, titanium, cobalt and nickel produced by this method have much better mechanical properties than the alloys produced by traditional methods [5, 6]. In aluminum-based alloys obtained by *SLM*, structural defects are easily formed, which lead to intense cracking. Scientists offer various ways to eliminate these defects. In the study [7], cracking was prevented by reducing the cooling rate during the *SLM* process and reducing heat transfer from the parts to the platform. Koutny et al. [8] investigated the influence of *SLM* process parameters (laser power, scanning speed, scanning strategy and platform heating) on the relative density and mechanical properties of specimens obtained from 2618 alloy (*Al-Cu-Mn-Mg-Ag* alloy) [3]. During the experiment the formation of cracks was observed in the specimens, due to the high temperature difference between the solid and liquid phases while solidifying. Reducing the thermal gradient due to the construction of supporting elements leads to a decrease in the number of cracks. Heating the platform to 400 °C and lower scanning speed could not improve the quality of the specimens and caused gas porosity. In a study by Reschetnik et al. it is said that the parts made of 7075 alloy (*Al-Zn5.5-Mg-Cu*) by the *SLM* method have low mechanical properties [9]. The reason for the reduced mechanical properties is cracking that occurs when hardening. The authors suggested changing the melting modes (laser power, scanning step and scanning speed) and further heat treatment to improve the mechanical properties.

New aluminum-based systems are currently being developed specially for additive manufacturing. In the paper [10], the problem of cracking of specimens made of aluminum 6061 alloy (*Al-Mg-Si-Fe-Cu-Mn-Cr-Zn-Ti*) was solved by adding zirconium oxide into the alloy as crystallization centers. The literature also describes that the light element magnesium significantly increases the strength of the aluminum matrix through the dispersion hardening mechanism, while scandium increases the strength of the aluminum matrix through grain refinement [11], [12].

Taking into consideration the significant increase in the amount of aluminum powders used in additive manufacturing, the *Aluminum Association* has developed an aluminum alloy registration system known as *Purple Sheets* [13]. Today, the prices for commercially available aluminum alloy powders for *SLM* vary within the range of 40–80 US dollars per kg, those for *Al-Si-Mg* alloys reach up to 200 US dollars per kg. The quality and spherical shape of the powder also affect the price: powders produced by plasma atomization are usually more expensive than powders produced by gas atomization [14, 15]. Because of this, at present, the cost of parts produced by *SLM* method is much higher than those manufactured by traditional methods. To reduce the cost of products and save material, the non-fused powder can be reused [14, 15], although reused powders include soot, combustion and oxidation products, which leads to deterioration of the mechanical properties of the parts [14, 16].

The growing number of alloys currently listed in *Purple Sheets* [13] indicates that there is demand for a wide range of aluminum alloys for additive manufacturing.

It is noted that optimal processing parameters are especially important for the wide use of *SLM* obtained aluminum alloys in industry [17]. This is mainly because aluminum powder has high reflectivity and high thermal conductivity, which reduces the laser absorption of the powder [18, 19]. In addition, the oxide layers formed on the melt pool promote the porosity formation [16]. Pores and defects in *SLM* manufactured parts usually worsen the mechanical properties of the products.

This work is aimed at synthesizing a composite powder of a circumspherical shape *Al-Si-Mg* (*Al* – 91 wt. %, *Si* – 8 wt. %, *Mg* – 1 wt. %) from powders of *PA-4* aluminum (GOST 6058-22), silicon (GOST 2169-69) and magnesium *MPF-4* (GOST 6001-79), which were not originally intended for selective laser melting technology, and optimization of *SLM* modes to produce an alloy and form three-dimensional specimens with minimal porosity and zero cracking [20]. To achieve this goal, it is necessary to complete the following tasks: to obtain a powder composition from the mixture of single-component powders with circumspherical particles; to determine the structural and phase composition of the resulting composition of powders using scanning electron microscopy, X-ray diffraction and X-ray phase analysis; to form the specimens using selective laser melting technology; to determine the optimal energy density to ensure minimum porosity of the specimens; to anneal the specimens; to determine the microhardness of the specimens before and after annealing; to study the structural-phase composition of the specimen using transmission microscopy.

Research methods

Single-component aluminum, silicon and magnesium powders were subjected to sieve analysis to obtain the *Al-Si-Mg* powder composition. Particles with the size of 20–64 μm are optimal for selective laser melting technology. The distribution of the fractional composition of aluminum powder is shown in figure 1.

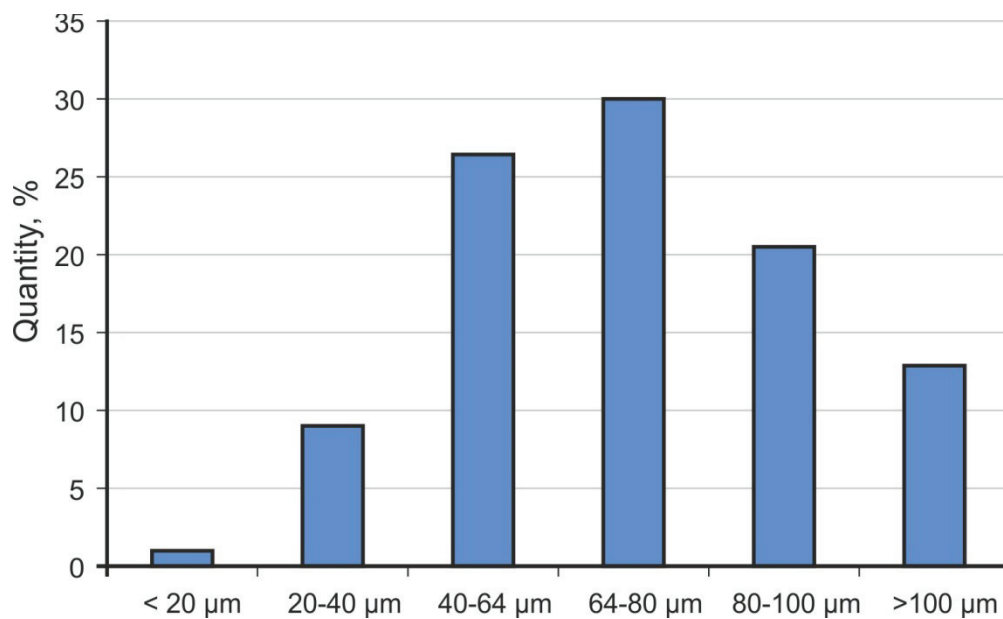


Fig. 1. Particle size distribution of *PA-4* powder (GOST 6058-22)

X-ray structural and X-ray phase analysis were performed on a *DRON-7* X-ray diffractometer (*Burevestnik*, Russia). Scanning electron microscopy was carried out on a *LEO EVO* scanning electron microscope at the *Nanotech Shared Use Center* [20].

Specimens with a size of $10 \times 10 \times 2$ mm were produced on a *VARISKAF-100MVS* 3D printer, which is equipped with a 100 W ytterbium fiber laser. The scanning speed *V* was chosen as the first variable factor of *SLM*: 225, 250, 275, 300 mm/s, the second variable factor was the scanning step *S*: 0.09, 0.08, 0.07 mm. The power of continuous laser radiation *P* was 90 W, the thickness of the powder layer *h* = 0.025 mm, the protective medium was argon, the temperature of the working table at the beginning of the *SLM* cycle was +25 $^{\circ}\text{C}$. Then the specimens were subjected to grinding and polishing with diamond pastes, removing the top layer of about 400 μm . Porosity was determined as the average of nine optical images of the polished section surface.

The specimens were annealed at a temperature of 400 $^{\circ}\text{C}$ for 5 hours.

The microhardness testing of the polished specimens was carried out using a *Duramin 5* model with the applied load of 50 g and the holding time of 10 s. To achieve average readings, a 10-point measurement mode was selected in longitudinal and cross sections.

The studies of the structural and phase state of the specimen were carried out using a *JEOL JEM-2100* transmission electron microscope.

Results and Discussions

Powders with the particle size of 20–64 μm were combined in the weight proportion of *Al* – 91 wt. %, *Si* – 8 wt. %, *Mg* – 1 wt. %, and then subjected to stirring in a ball mill for one hour in the protective atmosphere of argon to prevent the formation of oxides and the undesirable effect of oxygen on the structure and phase composition of the resulting powder [20]. Exploratory experiments showed that the time of mechanical alloying equal to 40 and 50 minutes is not enough to obtain a circumspherical shape. Therefore, all further studies were carried out with a powder composition subjected to 60 minute activation.

The following is a brief description of the results obtained when working with X-ray diffraction patterns of *Al-Mg-Si* powder specimens obtained by mechanical stirring in a ball mill working on the “tumbling drum” principle for 1 hour.

X-ray diffraction shows the identification of aluminum, silicon and magnesium phases (figure 2). The phase composition of aluminum was established as 91 %, that of silicon was established as 8 % and that of magnesium was established as 1 %.

Fig. 3 shows scanning electron images of the mixed aluminum, silicon and magnesium powder. The powder composition is a conglomerate of circumspherical particles and irregularly shaped satellites with particle sizes from 1 to 170 μm (figure 3 a). The elemental composition of particles is as follows: aluminum (90.3 wt. %), silicon (8.4 wt. %) and magnesium (1.3 wt. %).

The enlarged image in figure 3, a shows powder particles with a predominantly smooth surface, fine grain structure and some fine satellite powders partially fused to the surface of the larger particles. The mapping method made it possible to determine the uniform distribution of aluminum powder particles in the form of large and small conglomerates throughout the entire volume of the mixture (figure 3, b). From the distribution map it was concluded that aluminum occupies the largest share in the powder mixture. Silicon powder is distributed non-uniformly throughout the volume of the powder mixture in the form of

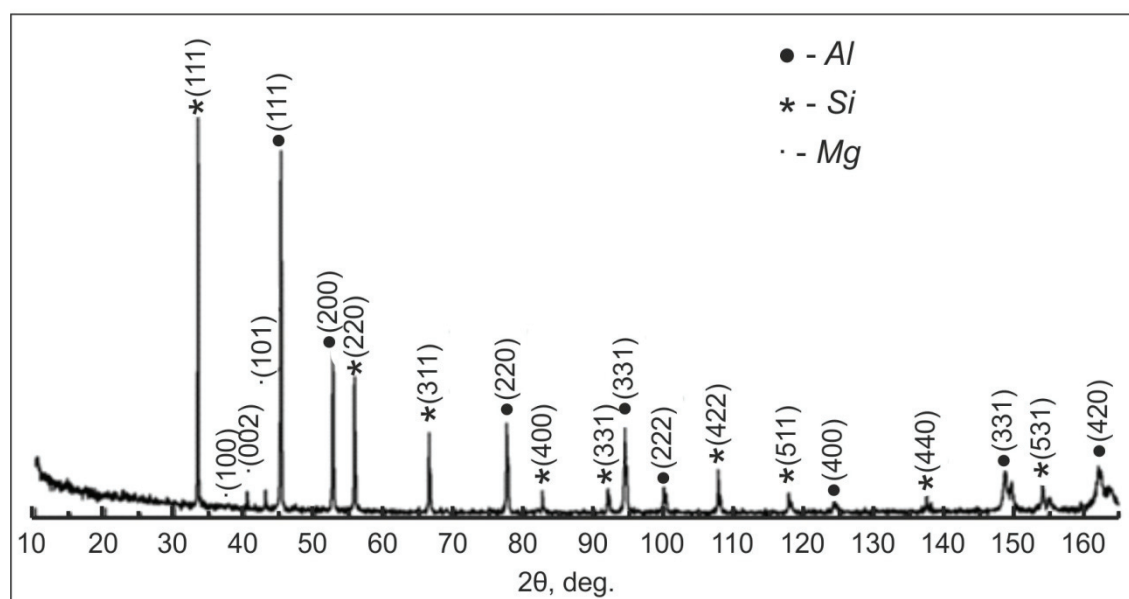


Fig. 2. X-ray diffraction pattern of a specimen of *Al-Si-Mg* powder obtained by stirring for 1 hour

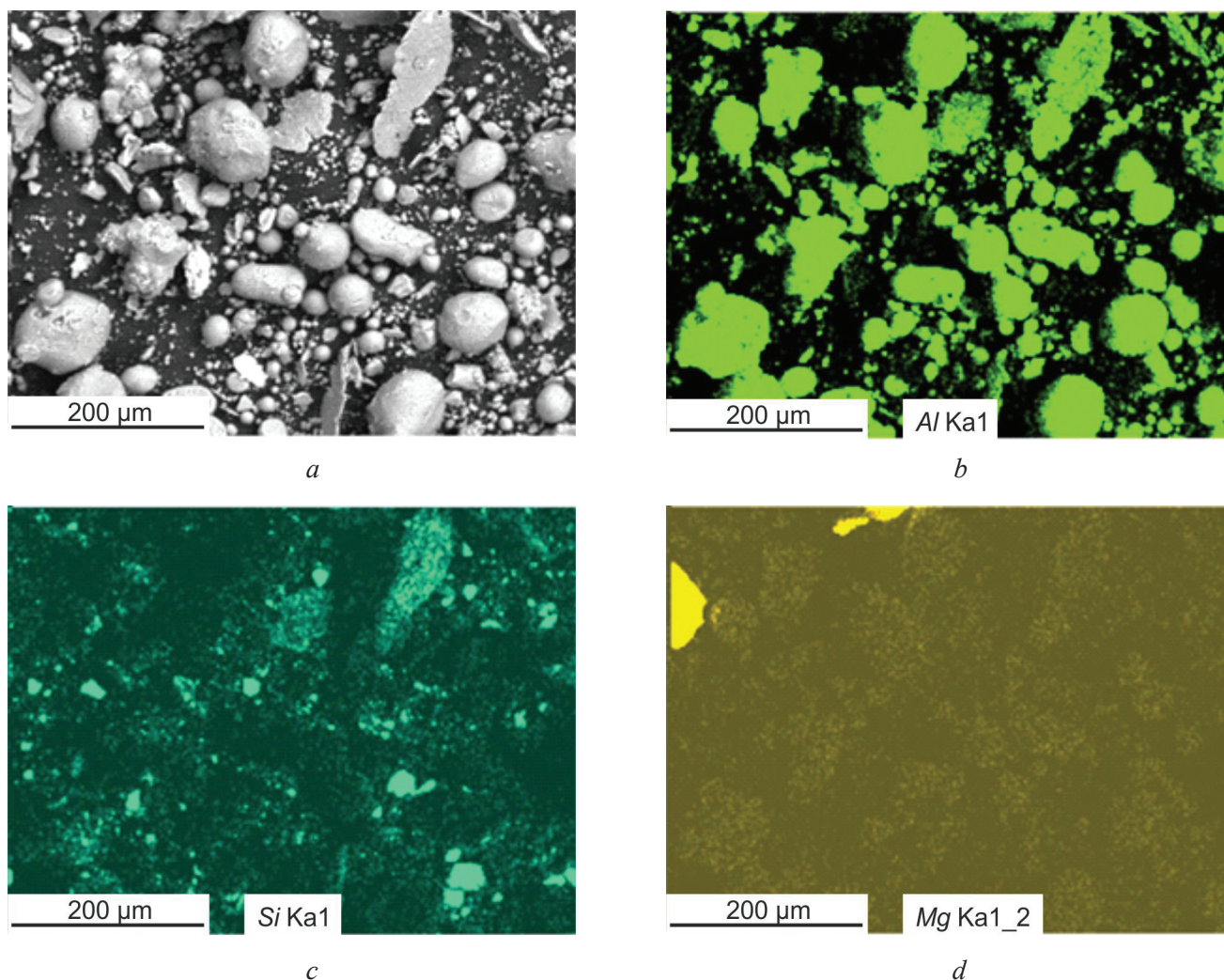


Fig. 3. SEM images (a) and distribution maps of the elements Al (b), Si (c), Mg (d), after 1 hour of mechanical activation

individual small particles ranging in size from 5 to 20 μm and is also present as a deposit of smaller particles on the surface of aluminum. Silicon is present in the smallest amount in the volume of the powder mixture, as can be seen on the corresponding distribution map (figure 3, d).

This fact is also confirmed by the completed elemental energy-dispersive microanalysis. The magnesium content in the volume of the powder mixture does not exceed 1.3 wt. % and 1.5 at. %. At the same time, the aluminum content in the powder composition is 90.3 wt. % and 90.8 at. %, and that of silicon is 8.4 wt. % and 7.7 at. %.

The specimens were produced from the composite powder using *VARISKAF-100MVS* unit. Based on the results of exploratory experiments, the following variable mode parameters were selected for further research: scanning speed: 225, 250, 275, 300 mm/s, scanning step: 0.09, 0.08, 0.07 mm; the constant parameters were as follows: continuous laser radiation power – 90 W, powder layer thickness – 0.025 mm, argon protective environment; the temperature of the working table at the beginning of the *SLM* cycle was +25 °C. Specimens with a size of 10×10×2 mm were made. At a scanning speed of 300 mm/s, the surface of the specimens showed an increase in porosity, so experiments were not carried out at 350 mm/s.

The table presents the photos of the structure of the specimen with minimal porosity of 0.03 %. The specimen was produced under the following *SLM* mode: $P = 90$ W; $V = 225$ mm/s; $S = 0.08$ mm; $h = 0.025$ mm; $T = 25$ °C. Porosity value was found as the average of nine measurements.

Porosity was determined in the same way at laser speed $V = 250, 275, 300$ mm/s.

Figure 4 shows the graph of the dependences of the porosity values on the scanning speed for the specimens obtained under the following *SLM* mode: $P = 90$ W; $h = 0.025$ mm; $T = 25$ °C.

Porosity values determined from a photograph of the structure of a specimen obtained by SLM from a composition of powders under the following SLM mode: $P = 90 \text{ W}$; $V = 225 \text{ mm/s}$; $S = 0.08 \text{ mm}$; $h = 0.025 \text{ mm}$; $T = 25 \text{ C}^\circ$

0.04	0.01	0.02
0.06	0.01	0.02
0.05	0.04	0.03
The average porosity value is 0.03 %, the energy density is $E = 200 \text{ J/mm}^3$		

Fig. 5 shows SEM images and elemental mapping of the specimens produced from the mixed aluminum, magnesium and silicon powders. The distribution maps of aluminum, magnesium and silicon show that the elements in the matrix are distributed uniformly over the entire surface of the specimens.

As a result of the study of the elemental composition, it was revealed that the elements in the specimen are distributed as follows: aluminum – 90.5 wt. % and 91 at. %, silicon – 7.8 wt. % and 8 at. %, magnesium – 1.7 wt. % and 1 at. %.

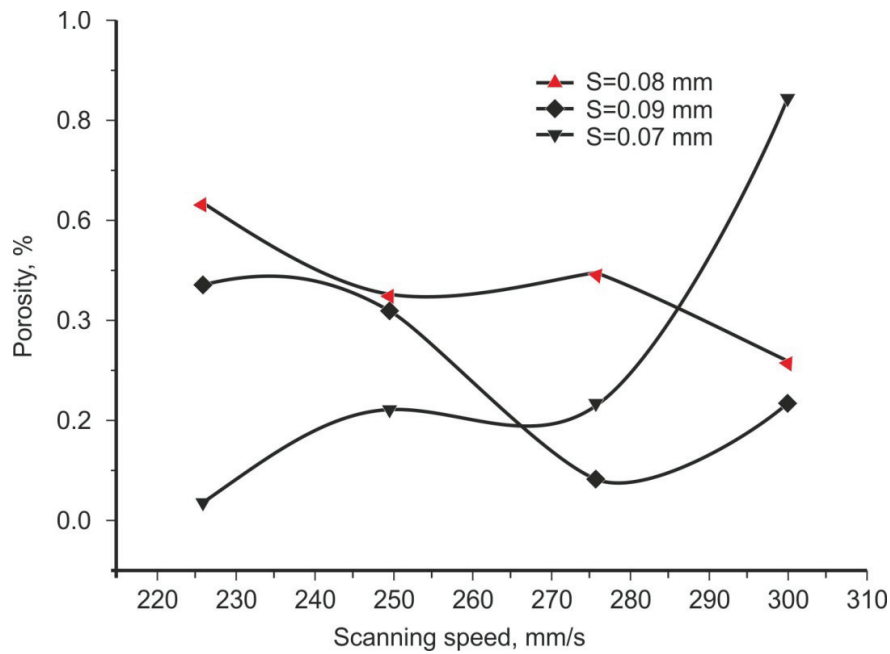
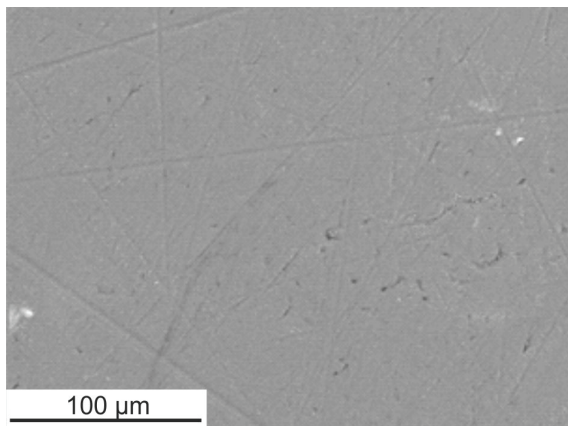
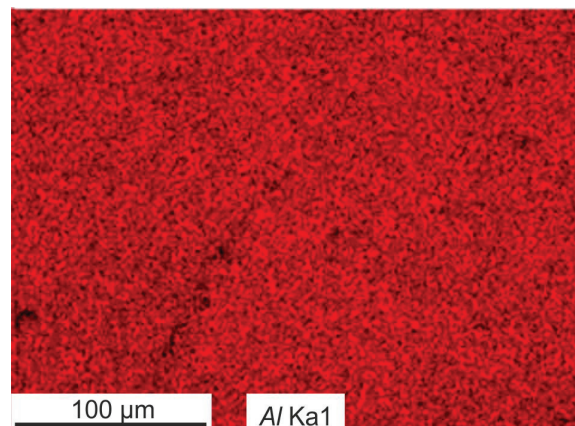


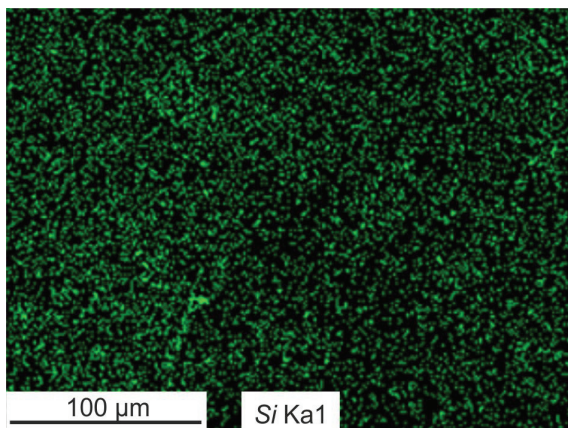
Fig. 4. Plot of the dependence of the average porosity value against the scanning speed and step of specimens obtained in SLM modes:
 $P = 90 \text{ W}$; $h = 0.025 \text{ mm}$; $t = 25 \text{ }^\circ\text{C}$



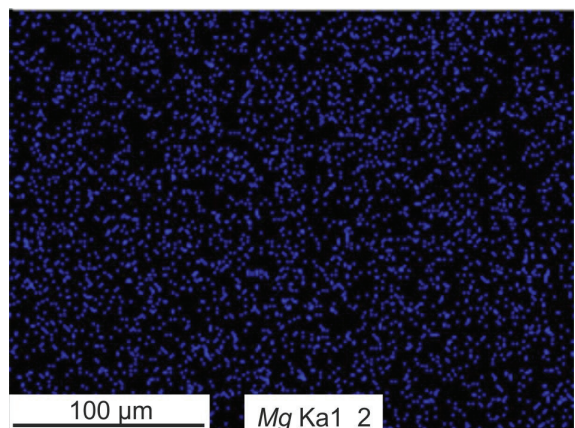
a



b



c



d

Fig. 5. SEM images of the surface of the specimen (a), formed by SLS from Al-Si-Mg powder and distribution maps of the elements Al (b), Si (c), Mg (d)

Analysis of the completed studies shows that powder mixing in the process of its mechanical activation contributes to the creation of bulk samples using selective laser melting with uniform distribution of powder elements (aluminum, silicon and magnesium).

Figure 6 presents the results of microhardness tests. The microhardness was measured at ten points in the longitudinal and cross sections of the specimen. The tests show that the specimen has an average microhardness value of 1,291 MPa in the longitudinal section, and that of 1,243 MPa in the cross section. The deviations of the values do not exceed 5 %.

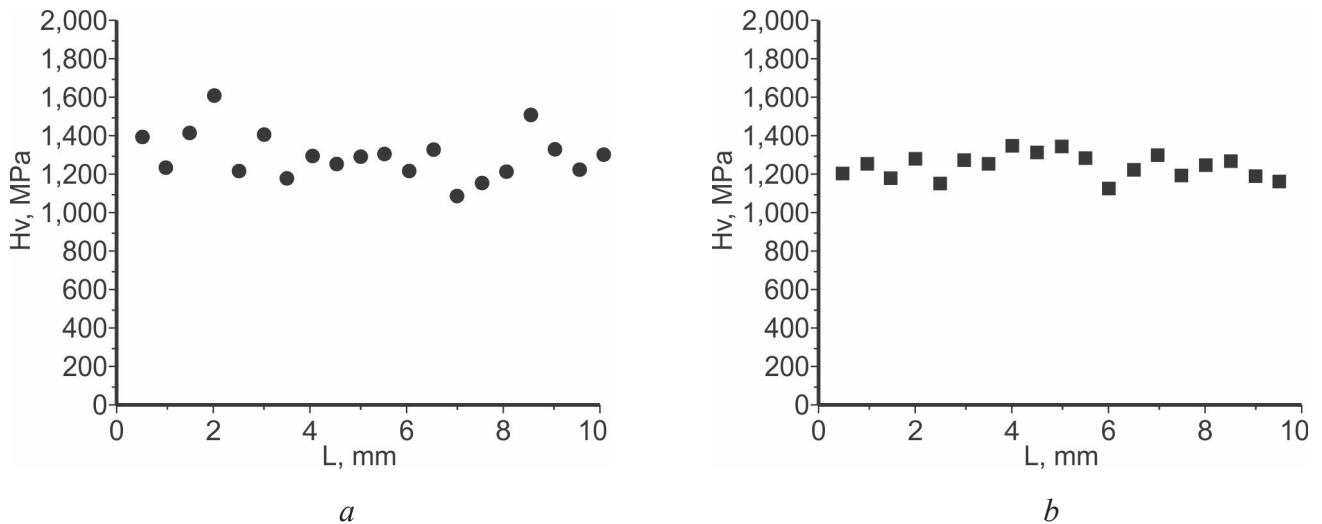


Fig. 6. Microhardness distribution over the *AlSiMg* specimen: in the long section of the specimen (a), in the cross section of the specimen (b)

The modes were selected and the specimens were annealed at a temperature of 400 °C for 5 hours to reduce residual stresses.

SEM images of the annealed specimens show that the surface is characterized by a uniform morphology without visible defects (figure 7). Annealing of the specimens leads to densification of the surface structure of the specimens.

Figure 8 shows *SEM* images and distribution maps of elements (*Al*, *Mg*, *Si*) of the specimens obtained after annealing. Aluminum and magnesium are distributed uniformly in all specimens. Silicon in the specimens is distributed in the form of small particles with the size of less than 5 μm.

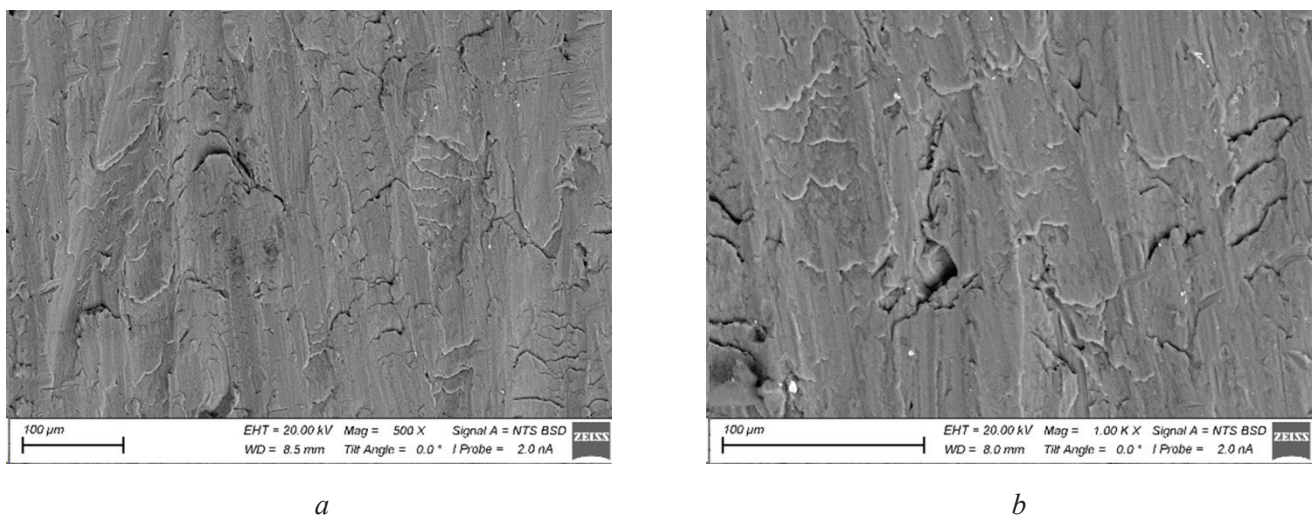


Fig. 7. *SEM* images of specimens before annealing (a), after annealing (b)

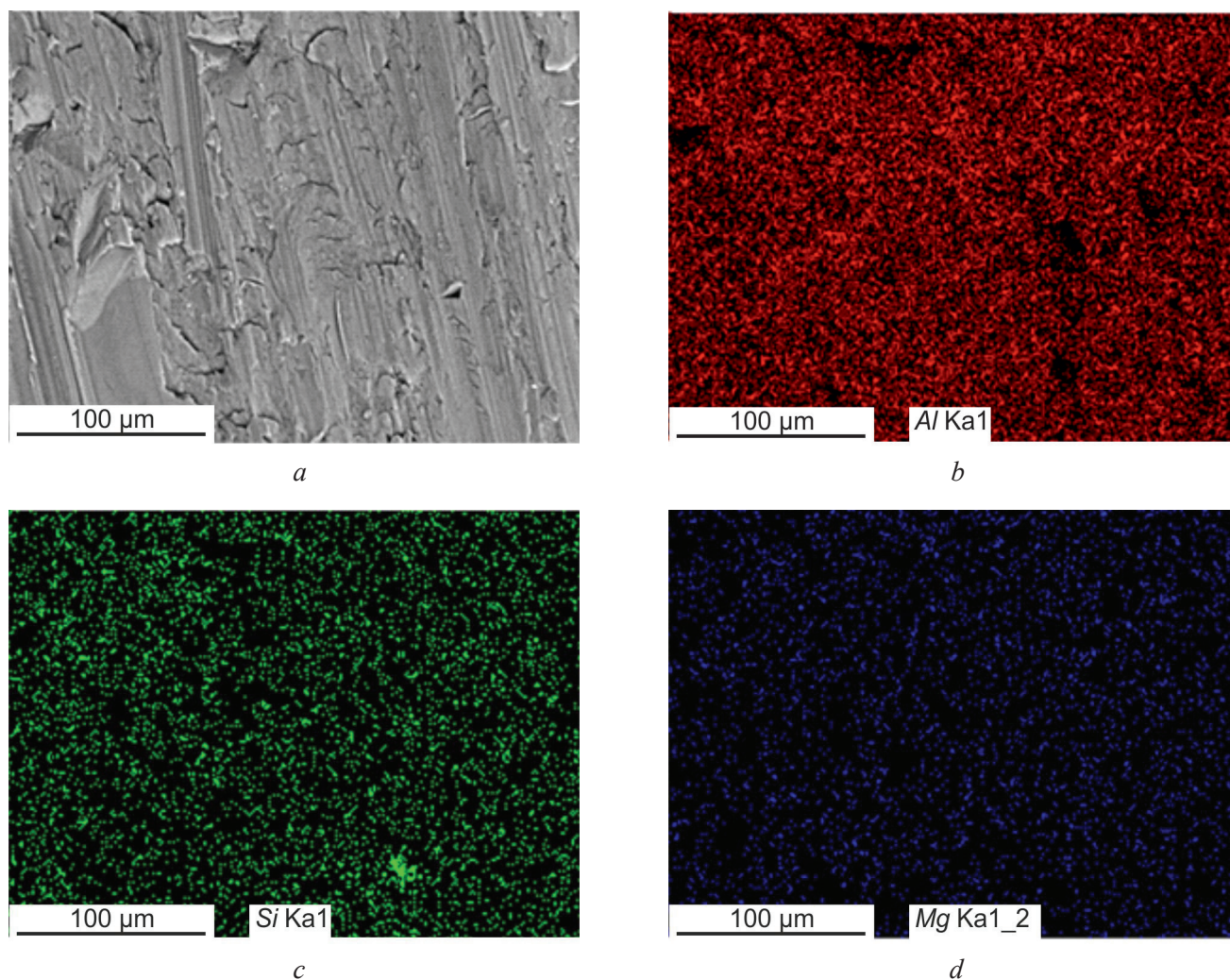


Fig. 8. SEM images and distribution maps of elements (*Al*, *Mg*, *Si*) of specimens after annealing

The elemental composition showed that the elements in the specimen are distributed as follows: aluminum – 88.6 wt. % and 88.2 at. %, silicon – 9.9 wt. % and 9.5 at. %, magnesium – 1.5 wt. % and 2.3 at. %.

The microhardness of the annealed specimen was 722 MPa in the longitudinal section and 710 MPa in the cross section. The decrease in microhardness by almost 50 % during the heat treatment strictly depends on the microstructural changes. All the studies reviewed note the decrease in strength after the heat treatment. In all the considered works, there is a decrease in strength after heat treatment, which becomes more intense with increasing temperature or duration of heat treatment. These changes in mechanical behavior follow quite directly from the gradual decrease of the supersaturation of α -*Al* matrix, rupture of the *Si* network and continuous growth of relatively large *Si* particles.

Studies of the structural-phase state of the specimen were carried out using a *JEOL JEM-2100* transmission electron microscope. It showed that the specimen under study had a grain structure, as can be seen in figure 9. Microscopic pores were not detected on the specimen under study in the area accessible for study with the magnifications used.

The given work showed that pre-prepared non-spherical powder materials can be used for selective laser melting. Formation of three-dimensional specimens with minimal porosity and absence of cracking by the *SLM* method from aluminum *PA-4* (GOST 6058-22), silicon (GOST 2169-69) and magnesium *MPF-4* (GOST 6001-79) powders, which were not originally intended for selective laser melting technology, has experimentally proven possible under certain modes. The *Al-Si-Mg* alloy is well processed using *SLM* within the established processing modes, where the constructed specimens can reach a material density of more than 99.7 % without cracking during solidification or large metallurgical defects.

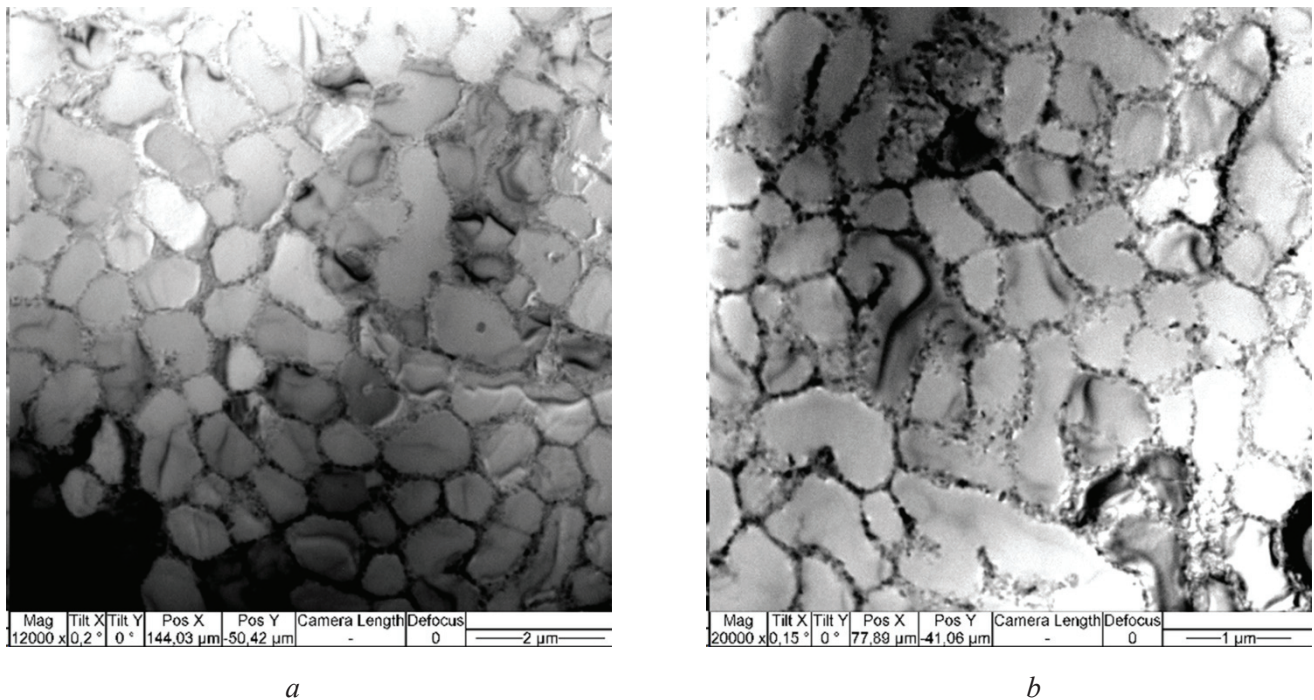


Fig. 9. Light-field images on various parts of the specimen

When a laser interacts with the powder composition, a number of complex physical and chemical phenomena occur on the surface of the specimen in the process of rapid melting and solidification. The phenomena include absorption and scattering of laser energy, heat transfer, phase transition and melt flow. The thermodynamic and kinetic behavior of the melt pool can be changed by adjusting the processing parameters. The work establishes optimal processing conditions including: laser power of 90 W, the scanning speed of 225 mm/s, the scanning step of $S = 0.08$ mm to make products from the powder composition with aluminum powder size of 20 to 64 μm . Porosity analysis revealed the area of high consolidation without significant metallurgical defects.

Less laser power result in reduced energy input causing disordered surface solidification due to low wettability of aluminum. The liquid phase is not enough to fill the cracks [17, 21]. High energy input is required for rapid propagation of heat and cooling due to the high thermal conductivity and high reflectivity of aluminum [19]. Increasing the laser power to 90 W and more improves the wettability of the powder and reduce the dynamic viscosity of the molten aluminum-based material [23]. As a result, the liquid melt fills the pores compacting the structure, which leads to optimal fusion.

The scanning speed is the second important parameter of the SLM mode; increasing it can significantly reduce the product manufacturing time. In experiments with the powder composition under consideration, its increase to 300 mm/s reduces the effect of laser energy on the processed layer of powder and its wettability, resulting in the gradual growth of porosity.

Setting the scanning speed of less than 225 mm/s and the laser power of more than 90 W leads to the growth of the thermal conductivity effect, but it also increases the cooling time. Long-term interaction between the laser and metal powder occurs under the low scanning speed and high power, and pores are formed [23]. In addition, increasing the laser power and decreasing the scanning speed enhances the evaporation of molten low-temperature materials, which leads to the change in the proportion of alloy elements, reduces the stability of the resulting fusion tracks and affects dispersion strengthening [24]. As a result, at the end of the laser scanning tracks there appear round pores filled with vapors or gases [17], which are trapped in the melt pool due to the non-equilibrium convection flow associated with ultra-high energy input.

For the samples built under the optimal conditions from the powder composition with aluminum powder size from 20 to 64 μm , the laser energy input was sufficient to achieve complete melting of the metal

powder, which resulted in high consolidation with an overall porosity level of less than 1%. There were no cracks in all samples.

To reflect the combined influence of laser power, scanning speed, scanning step and layer thickness on the material density the energy input E_V was calculated by the following formula [25]:

$$E_V = P/V h S$$

where P is the laser power (W), V is the scanning speed (mm/s), s is the scanning step (mm), h is the thickness of the powder layer (mm).

The energy density for obtaining specimens from the powder composition with aluminum measuring 20–64 μm with minimal porosity is 200 J/mm^3 .

Conclusion

Thus, the conditions for obtaining a powder composition and processing modes for producing a *SLM Al-Si-Mg* alloy were systematically studied and the optimal processing *SLM* range was established. The influence of the *SLM* mode on porosity and microhardness was also studied. The following conclusions can be made.

From metal powders that are not suitable for processing by selective laser melting, it is possible to obtain a powder composition with circumspherical particles, recommended for use in *SLM* units. Powders with the particle size of 20–64 μm were combined in the weight proportion of *Al* – 91 wt. %, *Si* – 8 wt. %, *Mg* – 1 wt. %, and then subjected to mixing in a ball mill for one hour in the protective argon atmosphere to prevent the formation of oxides and the undesirable effect of oxygen on the structure and phase composition of the resulting powder. The time of mechanical alloying equal to 40 and 50 minutes is not enough to obtain a circumspherical shape.

Analysis of the X-ray diffraction pattern of the powder composition allowed us to identify the phases of aluminum, silicon and magnesium. The phase composition was established as follows: aluminum – 91 %, silicon – 8 % and magnesium – 1 %.

SEM images of the powder composition produced after mechanical mixing for one hour showed that spherical particles and irregularly shaped satellites with particle sizes from 1 to 170 μm predominate in the powder.

The optimal *SLM* mode for forming a specimen with the minimal porosity of 0.03 % from an *Al-Si-Mg* alloy is as follows: laser power of 90 W, scanning speed of 225 mm/s, scanning step $S = 0.08$ mm, powder layer thickness of 0.025 mm, argon protective medium. The temperature of the working table at the beginning of the *SLM* cycle was +25 °C. The energy density is 200 J/mm^3 .

The relative density of materials produced in this range exceeds 99.7 %. There are no cracks.

The microhardness of the finished specimens is in the range from 1.243 to 1.291 MPa.

SEM images and distribution maps of the elements in the specimens produced from aluminum, magnesium and silicon powders showed that the elements are distributed uniformly over the entire synthesized surface.

The specimens annealed under the temperature of 400 °C for 5 hours have a more dense structure, while the microhardness decrease by almost 50 %. Optimal heat treatment conditions need to be further studied.

Studies of the structural-phase state of the specimen using transmission electron microscopy showed that the specimen under study has a dense grain structure.

References

1. Bandyopadhyay A., Heer B. Additive manufacturing of multi-material structures. *Materials Science and Engineering: R*, 2018, vol. 129, pp. 1–16. DOI: 10.1016/j.mser.2018.04.001.
2. DebRoy T., Wei H.L., Zuback J.S., Mukherjee T., Elmer J.W., Milewski J.O., Beese A.M., Wilson-Heid A., De A., Zhang W. Additive manufacturing of metallic components – process, structure and properties. *Progress in Materials Science*, 2018, vol. 92, pp. 112–224. DOI: 10.1016/j.pmatsci.2017.10.001.

3. Brice C.A., Tayon W.A., Newman J.A., Kral M.V., Bishop C., Sokolova A. Effect of compositional changes on microstructure in additively manufactured aluminum alloy 2139. *Materials Characterization*, 2018, vol. 143, pp. 50–58. DOI: 10.1016/j.matchar.2018.04.002.
4. Foteinopoulos P., Papacharalampopoulos A., Stavropoulos P. On thermal modeling of additive manufacturing processes. *CIRP Journal of Manufacturing Science and Technology*, 2018, vol. 20, pp. 66–83. DOI: 10.1016/j.cirpj.2017.09.007.
5. Khimich M.A., Ibragimov E.A., Tolmachev A.I., Saprykina N.A., Saprykin A.A., Sharkeev Y.P. Influence of thermal treatment duration on structure and phase composition of additive Co-Cr-Mo alloy samples. *Letters on Materials*, 2022, vol. 12 (1), pp. 43–48. DOI: 10.22226/2410-3535-2022-1-43-48.
6. Saprykin A.A., Sharkeev Y.P., Saprykina N.A., Ibragimov E.A. The mechanism of forming coagulated particles in selective laser melting of cobalt-chromium-molybdenum powder. *Key Engineering Materials*, 2020, vol. 839, pp. 79–85. DOI: 10.4028/www.scientific.net/KEM.839.79.
7. Karg M.C.H., Ahuja B., Wiesenmayer S., Kuryntsev S.V., Schmidt M. Effects of process conditions on the mechanical behavior of aluminum wrought alloy EN AW-2219 (AlCu6Mn) additively manufactured by laser beam melting in powder bed. *Micromachines*, 2017, vol. 8 (1), p. 11. DOI: 10.3390/mi8010023.
8. Koutny D., Palousek D., Pantelejev L., Hoeller C., Pichler R., Tesicky L., Kaiser J. Influence of scanning strategies on processing of aluminum alloy EN AW 2618 using selective laser melting. *Materials*, 2018, vol. 11 (2), p. 298. DOI: 10.3390/ma11020298.
9. Reschetnik W., Brüggemann J.P., Aydinöz M.E., Grydin O., Hoyer K.P., Kullmer G., Richard H.A. Fatigue crack growth behavior and mechanical properties of additively processed EN AW-7075 aluminum alloy. *Procedia Structural Integrity*, 2016, vol. 2, pp. 3040–3048. DOI: 10.1016/j.prostr.2016.06.380.
10. Martin J.H., Yahata B.D., Hundley J.M., Mayer J.A., Schaedler T., Pollock T.M. 3D printing of high-strength aluminum alloys. *Nature*, 2017, vol. 549, pp. 365–369. DOI: 10.1038/nature23894.
11. Otani Y., Kusaki Y., Itagaki K., Sasaki S. Microstructure and mechanical properties of 7075 alloy with additional Si fabricated by selective laser melting. *Materials Transactions*, 2019, vol. 60 (10), pp. 2143–2150. DOI: 10.2320/matertrans.Y-M2019837.
12. Sales R.C., Felipe P., Paradela K.G., Garcao W.J.L., Ferreira A.F. Effect of solidification processing parameters and silicon content on the dendritic spacing and hardness in hypoeutectic Al-Si alloys. *Materials Research*, 2018, vol. 21 (6), p. 8. DOI: 10.1590/1980-5373-mr-2018-0333.
13. Smith P., Cowie J., Weritz J. Registration system for aluminum alloys used in additive manufacturing. *Light Metal Age*, 2019, vol. 77 (4), pp. 72–75.
14. Moghimian P., Poirié T., Habibnejad-Korayem M., Zavala J.A., Kroeger J., Marion F., Larouche F. Metal powders in additive manufacturing: a review on reusability and recyclability of common titanium, nickel and aluminum alloys. *Additive Manufacturing*, 2021, vol. 43, p. 102017. DOI: 10.1016/j.addma.2021.102017.
15. Aboulkhair N.T., Simonelli M., Parry L., Ashcroft I., Tuck C., Hague R. 3D printing of aluminium alloys: additive manufacturing of aluminium alloys using selective laser melting. *Progress in Materials Science*, 2019, vol. 106, p. 100578. DOI: 10.1016/j.pmatsci.2019.100578.
16. Shen H., Rometsch P., Wu X., Huang A. Influence of gas flow speed on laser plume attenuation and powder bed particle pickup in laser powder bed fusion. *Materials Science & Engineering*, 2020, vol. 72, pp. 1039–1051. DOI: 10.1007/s11837-020-04020-y.
17. Bian L., Shamsaei N., Usher J.M., eds. *Laser-based additive manufacturing of metal parts: modeling, optimization, and control of mechanical properties*. Boca Raton, CRC Press, 2017. 328 p. ISBN 9781498739986.
18. Aboulkhair N.T., Everitt N.M., Maskery I., Ashcroft I., Tuck C. Selective laser melting of aluminum alloys. *MRS Bulletin*, 2017, vol. 42, pp. 311–319. DOI: 10.1557/mrs.2017.63.
19. Thijs L., Kempen K., Kruth J.P., Van Humbeeck J. Fine-structured aluminium products with controllable texture by selective laser melting of pre-alloyed AlSi10Mg powder. *Acta Materialia*, 2013, vol. 61, pp. 1809–1819. DOI: 10.1016/j.actamat.2012.11.052.
20. Saprykina N.A., Chebodaeva V.V., Saprykin A.A., Sharkeev Y.P., Ibragimov E.A., Guseva T.S. Synthesis of a three-component aluminum-based alloy by selective laser melting. *Obrabotka metallov (tekhnologiya, oborudovanie, instrumenty) = Metal Working and Material Science*, 2022, vol. 24, no. 4, pp. 151–164. DOI: 10.17212/1994-6309-2022-24.4-151-164.
21. Yap C.Y., Chua C.K., Dong Z.L., Liu Z.H., Zhang D.Q., Loh L.E., Sing S.L. Review of selective laser melting: materials and applications. *Applied Physics Reviews*, 2015, vol. 2 (4), p. 041101. DOI: 10.1063/1.4935926.



22. Li R., Wang M., Yuan T., Song B., Chen C., Zhou K., Cao P. Selective laser melting of a novel Sc and Zr modified Al-6.2 Mg alloy: processing, microstructure, and properties. *Powder Technology*, 2017, vol. 319, pp. 117–128. DOI: 10.1016/j.powtec.2017.06.050.

23. Han X., Zhu H., Nie X., Wang G., Zeng X. Investigation on selective laser melting AlSi10Mg cellular lattice strut: molten pool morphology, surface roughness and dimensional accuracy. *Materials (Basel)*, 2018, vol. 11, p. 392. DOI: 10.3390/ma11030392.

24. Zhang J., Song B., Wei Q., Bourell D., Shi Y. A review of selective laser melting of aluminum alloys: processing, microstructure, property and developing trends. *Journal of Materials Science & Technology*, 2019, vol. 35, pp. 270–284. DOI: 10.1016/j.jmst.2018.09.004.

25. Read N., Wang W., Essa K., Attallah M.M. Selective laser melting of AlSi10Mg alloy: process optimisation and mechanical properties development. *Materials & Design*, 2015, vol. 65, pp. 417–424. DOI: 10.1016/j.matdes.2014.09.044.

Conflicts of Interest

The authors declare no conflict of interest.

© 2024 The Authors. Published by Novosibirsk State Technical University. This is an open access article under the CC BY license (<http://creativecommons.org/licenses/by/4.0>).

